KuROS: A new airborne Ku-band Doppler radar for observation of the ocean surface

Danièle Hauser, Gérard Caudal, Christophe Le Gac, René Valentin, Lauriane Delaye, Céline Tison

KUROS : A NEW AIRBORNE KU-BAND DOPPLER RADAR FOR OBSERVATION OF THE OCEAN SURFACE

Danièle Hauser[1,2,3], Gérard Caudal[1,2,3], Christophe Le Gac[1,2,3], René Valentin[1,2,3], Lauriane Delaye[1,2,3] , Céline Tison [4]

(1) Université Versailles St-Quentin, (2) UPMC Univ. Paris 06, (3) CNRS/INSU, LATMOS-IPSL
(4) Centre National d'Etudes Spatiales
daniele.hauser@latmos.ipsl.fr

ABSTRACT

We have designed and developed a new airborne Ku-band Doppler radar, called KuROS, to prepare the CFOSAT satellite mission for measuring ocean surface wind and waves. The main characteristics of this new radar are presented, and first results obtained from a campaign held in 2013 illustrated. Both intensity and Doppler information are used to estimate the directional spectra of ocean waves. Radar cross-section and directional spectra are assessed trough comparisons with independent information.

Index Terms— Ocean waves, radar, scatterometer

1. INTRODUCTION

With the aim of preparing the future CFOSAT (China-France Oceanic satellite) satellite mission [1], we developed a new airborne radar, called KuROS (Ku-band Radar for Observation of Surfaces). CFOSAT will embark two instruments: SWIM (designed and manufactured by France), a Ku-Band wave scatterometer (incidence angles between 0 to 10°) aimed at measuring the ocean directional wave spectra, and SCAT (designed and manufactured by China), a Ku-Band wind scatterometer (wide swath around 40°) to provide the surface wind vectors. Details on CFOSAT and pre-launched SWIM performance analysis may be found in [1] and [2], respectively. The primary aim of KuROS is to optimize the choices made in the CFOSAT payloads and ground segment, and to serve as a tool for the geophysical validation of the CFOSAT geophysical products once launched. So, the KuROS specifications have been chosen to cover the geometry of both SWIM and SCAT. Another important objective of KuROS is to explore the characteristics of the kinematics of the sea surface. For this purpose, in addition to measuring the normalized radar cross section σ_0, KuROS has the ability to measure the Doppler velocity of the radar echo.

2. INSTRUMENT CHARACTERISTICS

KuROS is an airborne Ku band (13.5 GHz) radar designed to cover a large range of incidence angles (0-50°) and azimuth angles (0-360°) in order to address the geometry of observations of the two payload instruments (SWIM and SCAT) of CFOSAT. In addition, a Doppler measurement capability has been designed for KuROS. The whole system is mounted in an ATR42 aircraft, operated by the SAFIRE unit ("Service des Avions Français Instrumentés pour la Recherche en Environnement"), and the conditions of use of KuROS are specified to allow measurements from flights from about 500 m to about 3000 m above the surface.

In order to address the question of measuring both wind and waves, the KuROS antenna system is composed on two printed-array antennae: a HH-pol low incidence (called LI) antenna pointed to 14° incidence with respect to nadir and the dual-pol (HH/VV) medium incidence (called MI), antenna pointed to 40° incidence. Both antennae have a ±10° elevation and ±4° azimuth one-way beam-width. This relatively large aperture is required to estimate ocean wave spectra from a real-aperture radar at small-incidence (see [3], [4]). Both antennae have been tested in anechoic chambers to determine their radiation patterns. However, when integrated within the body of the aircraft, it turned out that the MI antenna pattern was not nominal. This is attributed to the presence of a metal collar used to adjust the antenna system within the body of the plane. This problem will be fixed for future campaigns by implementing a new interface. Meanwhile, the results presented in this paper are focused on the observations performed with the LI antenna. The antenna system can be controlled either to rotate over 360° around the vertical axis at a variable rotation speed, or to stop at a fixed azimuth angle.

The bandwidth has been chosen in order to achieve a high range and horizontal resolution: 100MHz for LI antenna and 30MHz for the MI antenna, corresponding respectively to a range resolution of 1.5m (close to the SWIM specification) and 5m,. Because of the large range of distances to be sampled (flight altitudes from 500m to 3500m, incidences from 0 to 50°), and some real-time constraints, several chronograms of transmitted pulses are used, depending on flight altitude and antenna. Typically for the LI antenna used from a 2000 m flight-level the pulse length and PRF are respectively 10.33 μs, and 35 kHz. All these modes are pre-loaded in the control unit and chosen by the operator during flights. At reception, after

going through the two switches and a circulator, the received chirps are sent to the low noise amplifier, and then filtered to limit the noise band and conserve only the upper band. The microwave signal is down converted with the same frequency source oscillator as used in the transmitter part. The signals are then amplified, filtered by an anti-aliasing filter and transmitted to the digital converter. As for the digital processing, after sampling the IF signal at 360 MHz, the range compression is obtained by multiplication by a replica signal, then the signal is re-sampled at 60 MHz. Then a FFT processing is applied to obtain amplitude and phase of the backscattered signal as a function of range. The last step is the real-time coherent integration of the complex samples over 1ms. We choose to use the pulse pair processing technique [5], which provides amplitude and phase of the mean signal with an efficient noise reduction. The radiometric data (I&Q signals integrated on 1ms) and the ancillary data (aircraft attitudes, GPS) are recorded at the same rate of 1 kHz.

Both internal and external calibrations (using corner reflectors for the latter) are used to ensure stability and absolute values of σ_0 (these latter specified with a minimum accuracy of 1 dB). Using pulse-pair integration over 33 ms during the ground processing a radiometric accuracy of 0.2 dB is obtained. Measurements over corner reflectors have also been used to assess the velocity estimates.

3. DATA SET, METHODS AND RESULTS

The first scientific data set of KuROS has been obtained during two campaigns held in 2013, namely the HyMeX campaign over the Gulf of Lion in the Mediterranean Sea [6] and the PROTEVS campaign near the coasts of Brittany (west of France). In 2013, KuROS has been successfully used for a total of 15 flights in different conditions of wind, waves, and current conditions (wind from 9 to 20 m/s, waves from 1.4 to 6.1 m significant wave height, tidal currents during PROTEVS up to 2 m/s). During each flight KuROS passed systematically over a meteo-oceanic buoy, which provides wind and wave spectra.

Processing includes estimate of σ_0 as a function of incidence and azimuth, after gain and geometry compensation. An example of mean σ_0 as a function of incidence is illustrated in Figure 1. It corresponds to a mean profile obtained over 33 ms and all azimuth angles, for a case of moderate wind speed (~9 m/s) and high sea-state (5.3 m significant wave height). The agreement with the models derived from TRMM radar [7,8] and with the NSCAT empirical model [9] in the same wind and wave conditions is reasonably good. This validates both our absolute calibration and the geometric corrections to account for aircraft attitude variations.

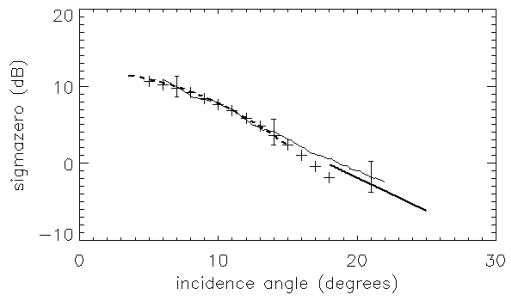

Figure 1: Normalized radar cross-section averaged over the azimuthal directions, as a function of incidence angle. Thin solid line : obtained from KuROS on 6 March 2013 (wind speed is 9m/s and significant wave height is 5.3m); the error bars indicate the standard deviation over an incidence angle bin of 1°. Dashed line : model from [7]. + signs : quadratic fit to TRMM data [8]. Thick solid line : NSCAT empirical model [9] .

KuROS is also designed to provide the directional spectrum of long ocean waves according to the method proposed by [3] and also used by [4]. The principle is to use a large footprint with respect to the waves to be measured and a high range resolution. Pointing the radar in the direction of the wave propagation, the backscattered signal is modulated by the slopes of the long waves (tilt modulation). At small incidences this modulation is linearly related to the local slopes of the waves. Modulations of radar reflectivity as a function of distance within the footprint are then spectrally analyzed to obtain the sea wave spectrum along the direction of observation, while the rotation of the antenna around the vertical axis permits to explore all the azimuthal directions. The theory is briefly recalled here (see [3] for details).

The elementary backscatter cross-section σ is given by $\sigma=\sigma_0 A$, where A is the area contained within a radar range gate. The fractional modulation of the cross section seen by the radar is $\delta\sigma/\sigma$ averaged laterally across the beam:

$$m(x,\varphi) = \frac{\int G^2(y)(\delta\sigma/\sigma)\,dy}{\int G^2(y)\,dy} \qquad (1)$$

where $G^2(y)$ is the two-way azimuth antenna gain pattern.

The sea wave polar-symmetric height spectrum $F(k,\varphi)$ is then obtained from the expression (cf [3], [4]):

$$F(k,\varphi) = \frac{L_y}{2\pi\ \cot\theta - \frac{\partial \ln\sigma_0}{\partial\theta}} \qquad (2)$$

where k, θ, and φ are wavenumber, incidence angle, and azimuth, respectively, L_y is a length related to the azimuthal width of the beam footprint, and $P_m(k,\varphi)$ is the modulation spectrum, defined as:

$$P_m(k,\varphi) = FT(m(x,\varphi)).\ FT^*(m(x,\varphi)) \qquad (3)$$

where *FT* refers to the Fourier transform operator, and * stands for complex conjugate.

As discussed in [3], the speckle noise of the radar technique produces an additional modulation of σ_0, included in the measured modulation spectrum. This speckle noise must be removed from the data to retrieve wave spectra. In order to estimate the spectrum of the speckle noise, [4] used a semi empirical method based on the comparison between data integrated over different time intervals. In the context of the processing of SAR images [10] proposed another approach, which consists to remove the speckle noise by computing image cross-spectra between pairs of single look SAR images separated in time. Following their approach, the modulation spectrum $P_m(k,\varphi)$ of equation (3) is replaced by the quantity:

$$P'_m(k,\varphi) = real\left\{FT(m(x,\varphi,t)).FT^*(m(x,\varphi,t+\delta t))\right\} \quad (4)$$

The time interval δt must be large enough so that the speckle noises of both profiles are uncorrelated, but small enough so that the radar resolution cell is only marginally displaced during that interval. Here we chose a time interval δt=66ms, which permits both conditions to be well fulfilled. The results obtained by this method are quite consistent with speckle estimates obtained using the approach described in [4]. The results presented below have been obtained by using this cross-spectral approach.

The slope spectrum of the surface waves $k^2 F(k,\varphi)$ is then obtained using Eq. (2), and the mean trend of σ_0 with incidence estimated from the observations (over the range {8°-18°}). In order to remove the 180° ambiguity in the propagation direction, we tested two methods based on the following principles, respectively: method 1: for each spectral component the sign of the real part of the cross-spectra between σ_0 modulations and surface velocity modulations gives the direction of propagation, because the velocity fluctuations are dominated by that of the orbital velocity of the waves; method 2: using a relatively long time lag between two observations (0.4s) the argument of their cross-spectrum provides the sign of the phase velocity of each wave spectral component after removing the aircraft velocity. By comparing with directional buoy data, we could conclude (not shown) that method 1 is more efficient than method 2 to remove 180° ambiguity. Fig. 1 shows an example of the directional spectra obtained using this method. Directional spectra of ocean waves contain information from different components related to different sources of generation (wind-waves generated locally, swell propagating from remote sites). Therefore it is essential to be able to distinguish different components in the 2D spectra. To do so, we have adapted a method based on a watershed partitioning algorithm [11] to take into account the noisy nature of the 2D spectra: while using the "watershed" method, we have applied noise reduction (averaging in wave number), discretization of energy levels, and an iterative scheme. The wave partition obtained on the case of Fig.1 is illustrated in Fig.2. The result is very consistent with the geophysical situation, as well as with buoy observations and model results: low energy wind waves propagating to North-West in agreement with wind temporary from South-east and two more energetic swell components (peak wavelengths of 170 m and 180m), propagating to west-southwest (250° and 230°) in agreement winds from East, North-East in the northern part of the basin. After integration of wave energy over azimuths, the omni-directional wave spectra can be compared to non-directional wave rider observations. Figure 3 illustrates the good consistency for all the coincident measurements of our 2013 campaign. Finally, Fig. 4 illustrates the performance of the significant wave height retrieval with KuROS compared to buoy measurements.

4. CONCLUSION

The first results obtained with the new airborne Doppler Ku-Band radar KuROS on ocean wave spectra and normalized radar cross-section at low to medium incidence have been shown to be very consistent. The fall-off of the normalized radar cross-section with incidence agrees with results from the literature. We have shown that the speckle-free wave directional spectra obtained by using the modulation transfer function according to [2] combined with profiles of σ° with incidence angles, are consistent with directional buoy observations, both in terms of significant wave height and principal parameters of the wavenumber spectrum (mean or peak frequency and direction). As concerns the issue of the 180° ambiguity removal, the method based on the correlation between modulations of σ° and modulation of Doppler velocity within the footprint is more efficient than the one based on the analysis of cross-spectra between successive modulations of σ° separated by some time lag. Partitioning of the 2D wave spectrum has been obtained using an improved "watershed" method. With these first results, we show that KuROS is a very useful tool for the preparation of the CFOSAT mission allowing tests of various algorithms and performance evaluation. Ongoing work concerns the analysis of speckle properties as a function of surface conditions (wind, waves) and geometry of observations, as well as analysis of the Doppler measurements. The very interesting data set of these first campaigns will also be used to study wind/wave and wave/current coupling at with a high spatial sampling (3 to 6 km). Finally, mean profiles of radar cross-section will be used to assess electromagnetic model and/or study statistical properties of short waves.

5. REFERENCES

1] Hauser D., C. Tison, J.-M. Lefevre, J. Lambin, T.Amiot, L. Aouf, F. Collard, and P. Castillan, *Proceedings of the ASME 2010 29th International Conference on Ocean, Offshore and Arctic*

engineering, Volume 4, Shanghai, China, 2010, pp. 85-90, doi : 10.1115/OMAE2010-20184, 2010.
[2] Tison C., T. Amiot, D. Hauser, T. Koleck, P. Castillan, N. Corcoral, Latest advances of the SWIM instrument, *Proceedings of IGARSS2014*
[3] Jackson F. C., W. T. Walton, and P. L. Baker, *J. Geophys. Res., Vol. 90,* 987-1004, 1985.
[4] Hauser D., G. Caudal, G. J. Rijckenberg, D. Vidal-Madjar, G. Laurent, and P. Lancelin, *IEEE Transactions on Geoscience and Remote Sensing, 30(5),* 981-995, 1992.
[5] Zrnic, D. S., , *IEEE Trans. Aerosp. Electron. Syst.,* Vol. AES-13, 344-354, 1977.
[6] Drobinski P., and 35 co-authors, *Bull. Amer. Meteorol. Soc., doi: http://dx.doi.org/10.1175/BAMS-D-12-00242.1 in press, 2013.*
[7] Freilich M. H., and B. A. Vanhoff, *Journal of Atmospheric and Oceanic Technology, Vol. 20,* 549-562, 2003
[8] Tran N., B. Chapron, and D. Vandemark, *IEEE Geoscience and Remote Sensing Letters, Vol. 4, No. 4*, 542-546, 2007
[9] Wentz F. J., and D. K. Smith, A model function for the ocean-normalized radar cross section at 14 GHz derived from NSCAT observations, *J. Geophys. Res., 104, No. C5,* 11,499-11,514, 1999
[10] Engen, G., and H. Johnsen, *IEEE Trans. Geosci. Rem. Sens., Vol. 33, No. 4,*1995
[11] Hanson J.L. and O.M. Phillips, *J. Atmos. And Oceanic Tech. vol18, 2001, p 277-293*

6. AKNOWLEDGEMENTS

The authors wish to thank technical staff at LATMOS in charge of the development and operations of Kuros. They also thank the SAFIRE team who operated the ATR42 aircraft, and the Technical Division of CNRS-INSU for its support in the radar on-board implementation design. IETR (from CNRS, Rennes Université, INSA, Supélec) designed and built the antennae. The buoy data have been provided by Meteo-France in the context of the HyMeX project. The development and operations of the Kuros radar was funded by the French space agency CNES (Centre National d'Etudes Spatiales) in the context of the CFOSAT mission preparation.

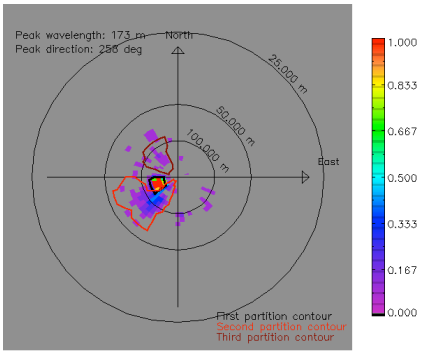

Figure 2:_ Directional sea wave slope spectrum obtained from a 30 s sample of KuROS observations. The ambiguity in the propagation direction has been removed using method 1. Energy density is in colour code, North-south and East-West wave number components are vertical and horizontal axis, in the meteo-oceanic convention.

Figure 3: Directional sea wave slope spectrum: same case and representation as in Fig2, but after applying a smoothing operation in wave number, and with the 3 identified partitions, sorted by decreasing energy (contours in black, red and brown). Wind direction at the time of measurement is 9 m/s from South-East.

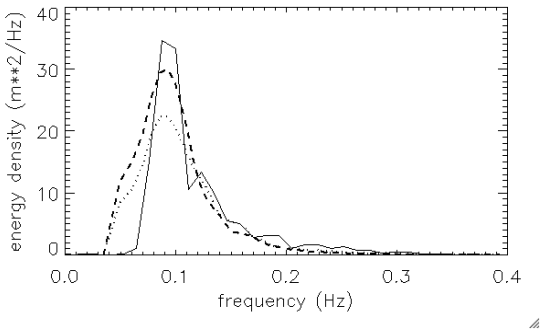

Figure 4:_ Omnidirectional sea wave frequency spectrum from the buoy (solid line) and from KuROS, just before and just after overflight of the buoy (resp. dotted and dashed lines)

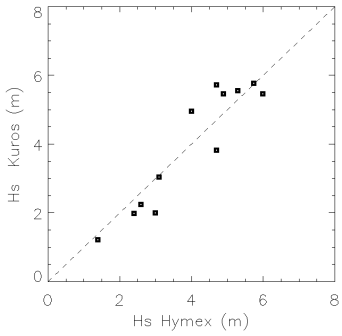

Figure 5: Significant wave heights from KuROS compared to the buoy measurements. The correlation coefficient is 0.93